ARTICLE

Efficient Technologies for the Fabrication of Dense TaB_2-Based Ultra-High-Temperature Ceramics

Roberta Licheri, Roberto Orrù,* Clara Musa, and Giacomo Cao*

Dipartimento di Ingegneria Chimica e Materiali, Unità di Ricerca del Consorzio Interuniversitario Nazionale per la Scienza e Tecnologia dei Materiali (INSTM), Unità di Ricerca del Consiglio Nazionale delle Ricerche (CNR), Dipartimento di Energia e Trasporti, Università degli Studi di Cagliari, Piazza D'Armi, 09123 Cagliari, Italy

ABSTRACT A 20 min ball-milling treatment (ball to powders ratio equal to 1) was demonstrated to be a valuable method for mechanochemically activating Ta, B_4C, Si, and graphite to prepare TaB_2−SiC and TaB_2−TaC−SiC ultrarefractory composites by self-propagating high-temperature synthesis (SHS). The resulting completely converted powders were spark plasma sintered at 1800 °C for 30 min, thus obtaining products about 96% dense. TGA characterization of bulk materials confirmed the beneficial effect of SiC in the resistance to oxidation behavior of the composite materials, while the presence of TaC appears to be unfavorable from this point of view. The obtained mechanical properties are in general comparable to those ones of Ta-based monolithic and composite bulk ceramics densified in previous works, although fracture toughness is significantly higher for TaB_2−SiC. This outcome holds also true when the comparison is extended to the TaB_2−TaC−SiC sample sintered in this work. The possible explanation is based on the occurrence of several toughening mechanisms (crack bridging, crack deflection, frictional interlocking, and crack branching) involved when TaB_2−SiC samples are subjected to the prescribed indentation conditions, whereas crack propagation is facilitated by the relatively finer and more homogeneous microstructure exhibited by the ternary system.

KEYWORDS: mechanical activation • self-propagating high-temperature synthesis • spark plasma sintering • ultra-high-temperature ceramics • tantalum diboride • tantalum carbide

1. INTRODUCTION

Melting temperatures higher than 3200 K, high hardness, high thermal and electrical conductivity, good chemical stability, thermal shock resistance, and resistance to ablation in oxidizing environments are the main interesting properties that make the class of materials known as ultra-high-temperature ceramics (UHTCs) suitable for several applications (1, 2). Specifically, metallurgy, microelectronics, refractory industries, and more recently, the aerospace field, where the fabrication of components that are exposed to high-flow environments like leading edges and nose caps in hypersonic re-entry vehicles is accounted for, represent potential markets where the exploitation of this family of ceramics could be advantageous (1−3).

In this context, despite their quite diverse applications, only a limited number of investigations have been devoted to refractory composites containing tantalum diboride (TaB_2) and monocarbide (TaC), as compared to the other, most widely investigated Zr- and Hf-based UHTCs (3). The presence of TaB_2 on the properties, mainly the oxidation resistance, of some refractory composites was studied by several authors (4−7). For instance, the oxidation resistance of ZrB_2−SiC materials was found to be significantly improved when ZrB_2 is partially replaced with tantalum diboride (4). In particular, the addition of 10 mol % TaB_2 was found to guarantee stronger protection to the modified composite when exposed to an oxidating environment at 1300 °C for 5 h, in comparison with the other additives tested, i.e., TiB_2, NbB_2, VB_2, and CrB_2.

More recently, further investigations of the influence of the TaB_2 content on the oxidation resistance of ZrB_2-based ceramics have been carried out (5, 7). The beneficial effect as a consequence of the addition of TaB_2 beyond 3.32 mol % was confirmed at 1200 and 1400 °C, whereas oxidation resistance was found to be relatively lower at 1500 °C. An improvement of this property was also evidenced when comparing the oxidative behavior of TaC−10 wt % TaB_2 with that of monolithic TaC (6). Bulk samples were obtained in this study by hot pressing (HP) at 2100 °C starting from TaB_2 synthesized by reducing Ta_2O_5 with B_4C and graphite in a tube furnace under Ar atmosphere, as described by the same authors in another paper (8). Another recent study involving this class of materials was focused on the use of the combustion synthesis as an alternative method for the preparation of TaB_2−TaC starting from Ta, B_4C and graphite (9). The initial mixture was preheated at 200 °C in order to make the process self-propagating upon ignition, because the synthesis reaction enthalpy is not sufficiently high.

In the present work, the fabrication of dense TaB_2−SiC (2:1 molar ratio) and TaB_2−TaC−SiC (4:4:1.5 molar ratio) composites is attempted for the first time taking advantage of a processing route successfully used in the past for the

* Corresponding author. E-mail: orru@dicm.unica.it (R.O.); cao@dicm.unica.it (G.C.). Phone: +39-070-6755076 (R.O.); +39-070-6755058 (G.C.). Fax: +39-070-6755057 (R.O.); +39-070-6755057 (G.C.).

Received for review March 12, 2010 and accepted June 5, 2010

DOI: 10.1021/am100211h

2010 American Chemical Society

Published on Web 06/21/2010

Table 1. Characteristics of the Starting Powders Used in the Present Investigation

powders	vendor	particle size (μm)	purity
Ta	Alfa-Aesar	<44	99.9%
B_4C	Alfa-Aesar	1−7	>99.4%
Si	Aldrich	<44	>99%
graphite	Aldrich	1−2	

obtainment of bulk MB_2−SiC and MB_2−MC−SiC (M = Zr, Hf) products (10−12). Such a method consists of first obtaining the refractory composite powders by mechanochemically activated self-propagating high-temperature synthesis (SHS) to be subsequently consolidated by an electric current activated sintering technique, namely the spark plasma sintering (SPS). The latter is a relatively novel technology where the powders and the die containing them are directly crossed by a pulsed current and simultaneously subjected to a mechanical load (13). It is generally established that the direct powder heating makes the SPS process significantly faster as compared to conventional HP, where the energy required for sintering is provided by an external heating source, thus requiring relatively longer processing times (typically on the order of hours) to reach acceptable relative density levels. The mechanochemical activation of the starting reactants is also taken into account in this study to sustain the combustion synthesis process of the UHTC powders. The bulk SPSed products are characterized in terms of microstructure, hardness, fracture toughness, and oxidation resistance and the results compared to those relative to analogous refractory materials.

2. MATERIALS AND METHODS

The characteristics of raw powders to be processed by SHS in the present investigation are reported in Table 1. Mixing of reactants was performed in agreement with the following reactions stoichiometry

$$2Ta + B_4C + Si \rightarrow 2TaB_2 + SiC \quad (1)$$

$$8\ Ta + 2B_4C + 1.5Si + 3.5C \rightarrow 4\ TaB_2 + 4\ TaC + 1.5SiC \quad (2)$$

Accordingly, TaB_2−27.9 vol % SiC (TS) and TaB_2−39.1 vol % TaC−13.7 vol % SiC (TTS) composites, respectively, are the expected desired products deriving from the complete conversion of the initial reactants.

Mechanochemical activation (MA) of the starting mixture was carried out by comilling reactants in a SPEX 8000 (SPEX CertiPrep, USA) shaker mill apparatus with two steel balls (13 mm diameter, 8 g weight) for 20 min milling time interval and ball to powders or charge ratio (CR) equal to 1.

Cylindrical pellets with a diameter of 10 mm, height of 30 mm and green density varying in the range of 50−62% of the theoretical values were prepared by uniaxially pressing about 10 g of mechanically activated powders. The synthesis process was conducted inside a reaction chamber under Ar atmosphere and initiated at one pellet end by using an electrically heated tungsten coil for few seconds. The temperature−time profile during SHS as well as the average velocity of the combustion wave were determined using W−Re thermocouples (127 μm diameter, Omega Engineering Inc.) embedded in the pellet. About 4 g of the obtained SHS product to be densified by SPS was first ground for 20 min using the mill apparatus described above equipped with a stainless steel vial and two steel balls (13 mm diameter, 8 g weight). Particle size distribution was determined by means of a laser light scattering analyzer (CILAS 1180, France).

The densification step of reacted powders was carried out under vacuum (10 Pa) using an SPS 515 equipment (Sumitomo Coal Mining Co. Ltd., Japan). The powders were first cold compacted into cylindrical graphite dies (outside diameter, 35 mm; inside diameter, 15 mm; height, 40 mm) lined with graphite foils (0.13 mm thick, Alfa Aesar, Karlsruhe, Germany) to protect the die and facilitate sample release after SPS.

All consolidation experiments were carried out at constant values of the dwell temperature, T_D = 1800 °C, mechanical pressure, P = 20 MPa, total sintering time, t_T = 30 min, heating rate equal to about 180 °C/min, and heating time, t_H = 10 min, i.e., the time required to reach the T_D value when starting from ambient temperature. For the sake of reproducibility, each experiment was repeated at least twice. Further details on the experimental procedure and setup used in this work can be found in previous works (10, 11, 14).

The relative density of the bulk products was determined using the Archimedes method. The theoretical densities of the corresponding composites, i.e., 9.98 (TS) and 12.05 (TTS) g/cm^3, were calculated through rule of mixtures (15) by considering the density values of TaB_2, TaC, and SiC as 12.6, 14.48, and 3.2 g/cm^3, respectively. A Philips PW 1830 X-rays diffractometer equipped with a Ni-filtered Cu K_α radiation (λ = 1.5405 Å) was used for phase identification. The microstructure and local phase composition of SHSed and SPSed end products were examined by scanning electron microscopy (SEM) (mod. S4000, Hitachi, Japan) and energy-dispersive X-rays spectroscopy (EDS) (Kevex Sigma 32 Probe, Noran Instruments, USA), respectively.

Vickers hardness and fracture toughness (K_{IC}) evaluation of the SPSed products was performed using a Zwick 3212 Hardness tester machine (Zwick & Co. GmbH, Germany) for 10 kg applied load with a dwell time of 18 s. In particular, the Palmqvist equation (16) was used for the evaluation of fracture toughness properties of TS and TTS samples.

Oxidation resistance was determined by thermogravimetric analysis (TGA) using a NETZSCH (Germany) STA 409PC Luxx Simultaneous DTA-TGA Instrument under 0.1 L/min air flow. Nonisothermal (dynamic) tests, consisting of slowly heating (2 °C/min) the specimen from room temperature to 1450 °C, as well as isothermal runs at 1450 °C for about 4 h, have been performed.

3. RESULTS AND DISCUSSION

3.1. Powders Activation, Synthesis, and Characterization. In contrast with the behavior displayed by the analogous Zr- and Hf-based systems recently investigated by combining the SHS and SPS routes (10−12), the synthesis reactions 1 and 2 did not exhibit a self-propagating character when starting from simply blended reactants. This outcome is justified on the basis of the corresponding enthalpies of reaction values reported in Table 2, significantly lower for the systems examined in this work. Thus, the heats of formation of TS and TTS are not high enough to sustain the propagation of the combustion wave after ignition and an appropriate activation method of reactants has to be identified to promote the synthesis process. This requirement is fulfilled in this work through the mechanical treatment of starting mixtures under the ball milling condi-

Table 2. Enthalpy of Formation of Different UHTC Systems (17)

system	$-\Delta H_r^\circ$ (kJ)
$2ZrB_2-SiC$	647.266
$2HfB_2-SiC$	674.042
$2TaB_2-SiC$	348.364
$4ZrB_2-4ZrC-1.5SiC$	2044.51
$3HfB_2-3HfC-SiC$	1727.573
$4TaB_2-4TaC-1.5SiC$	1380.762

tions reported in the Materials and Methods Section. Consequently, after reaction ignition, the synthesis process proceeded rapidly through the activated mixture while displaying average front velocity values of 4.5 ± 0.5 and 5.7 ± 0.4 mm/s for the case of the processed binary and ternary systems, respectively. Correspondingly, the maximum combustion temperatures measured during SHS were about 1850 and 2000 °C, respectively.

The need of reactant activation manifested in this work is in agreement with the behavior recently observed during the preparation by SHS of a similar composite, i.e., the TaB_2-TaC (9). In this case, the SHS character in the combustion synthesis process was induced by preheating at 200 °C the starting Ta, B_4C, and graphite reactants.

The diffraction patterns of the SHS products obtained in our study are reported in Figures 1 and 2 for the TS and TTS systems, respectively, along with those of the corresponding original reactants before and after their mechanical activation. A slight peak broadening, as an indication of crystal size refinement and internal strain increase, is the only effect evidenced by XRD analysis of the reactants powders after ball milling. The corresponding enhancement in chemical reactivity is a well-known effect mainly ascribed to the formation of interfaces among reactants during milling, which allows us to overcome the diffusion limitations that initially inhibit the self-propagation of the synthesis reaction (18).

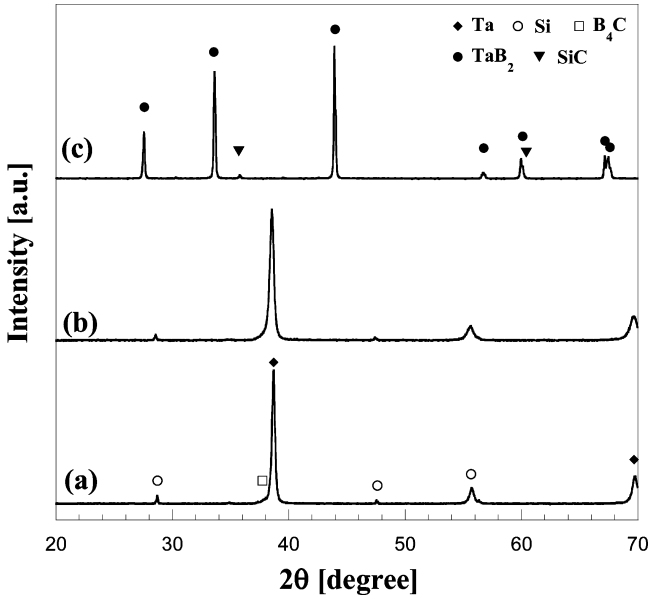

FIGURE 1. Comparison of XRD patterns of (a) original reactants, (b) mechanochemically activated reactants and (c) TS product obtained by MA-SHS according to reaction 1.

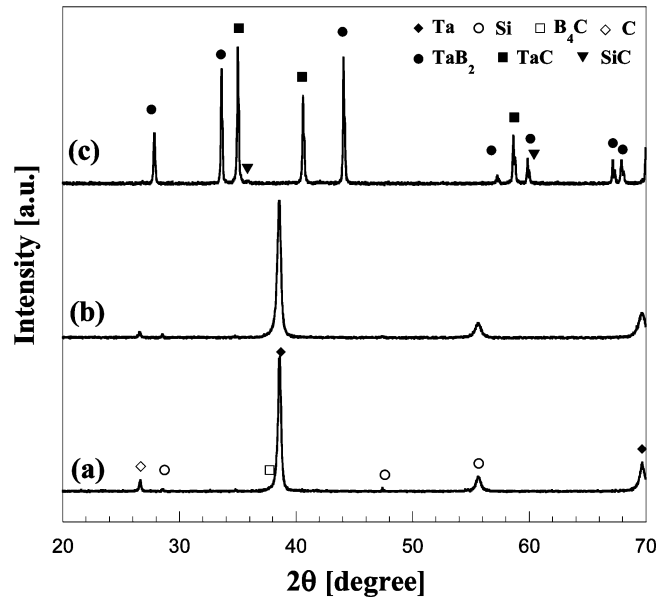

FIGURE 2. Comparison of XRD patterns of (a) original reactants, (b) mechanochemically activated reactants, and (c) TTS product obtained by MA-SHS according to reaction 2.

The XRD spectra of final products shown in Figures 1 and 2 clearly indicate that all peaks present in the patterns correspond only to the expected phases according to reactions 1 and 2. Therefore, it is apparent that the MA treatment allows SHS not only to occur but also to reach completion with the formation of the desired composite constituents.

Particle size distribution and microstructure of the obtained MA-SHS products were examined after being pulverized and before the consolidation stage. The cumulative curve obtained for the case of the TTS product is reported in Figure 3a, which shows that particle size was less than 40 μm. In addition, for the same system, it was found $d_{50} = 1.17 \pm 0.08$ μm. Moreover, the corresponding SEM-EDS analysis (cf. Figure 3b) evidenced that the majority of SHS powder particles are few micrometers in size and consist of TaC (brighter phase), TaB_2 (medium bright), and SiC (darker) fine mixed grains. Similar results are obtained for the case of the binary TS system. Specifically, in this latter case particle size was less than 30 μm and $d_{50} = 1.19 \pm 0.09$ μm.

3.2. Spark Plasma Sintering of MA-SHS Powders. On the basis of the results obtained in previous studies where the consolidation of similar composites, i.e., ZrB_2-SiC (10), $ZrB_2-ZrC-SiC$ (11), HfB_2-SiC and $HfB_2-HfC-SiC$ (12), by SPS was addressed, the densification of TS and TTS powders was also conducted for a total sintering time, $t_T = 30$ min, when setting the dwell temperature level (T_D) equal to 1800 °C, heating rate of about 180 °C/min, mechanical pressure $P = 20$ MPa, and the nonisothermal heating time $t_h = 10$ min.

An example of typical outputs recorded during the SPS process of TTS is reported in Figure 4 where sample shrinkage and temperature time profiles (Figure 4a) are shown along with the corresponding temporal current and voltage mean values (Figure 4b). The most remarkable displacement change was observed to occur in the time interval 7−9.5 min from the beginning of the current application, when the

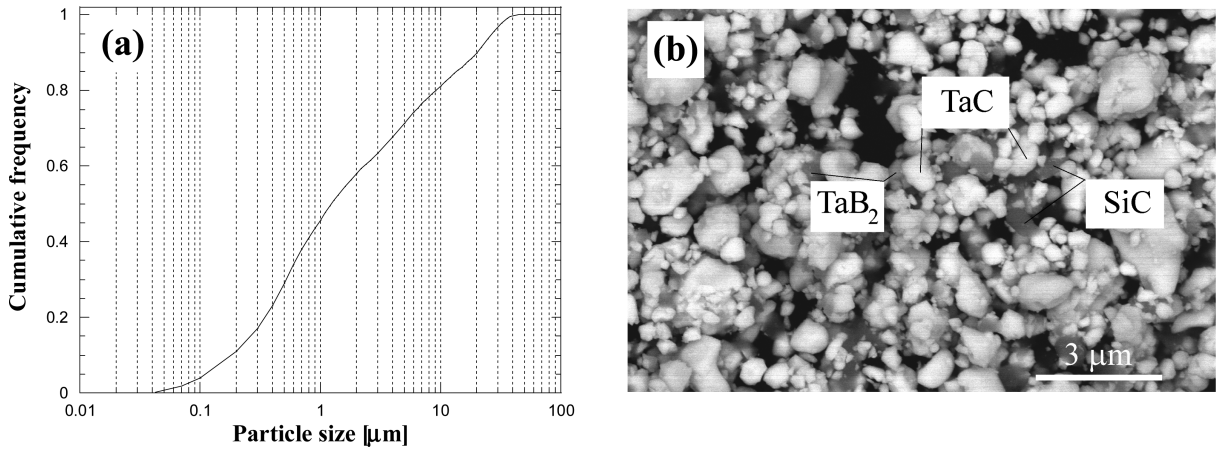

FIGURE 3. (a) Size distribution and (b) SEM backscattered micrograph of TaB_2−TaC−SiC powders obtained by MA-SHS after 20 min ball milling.

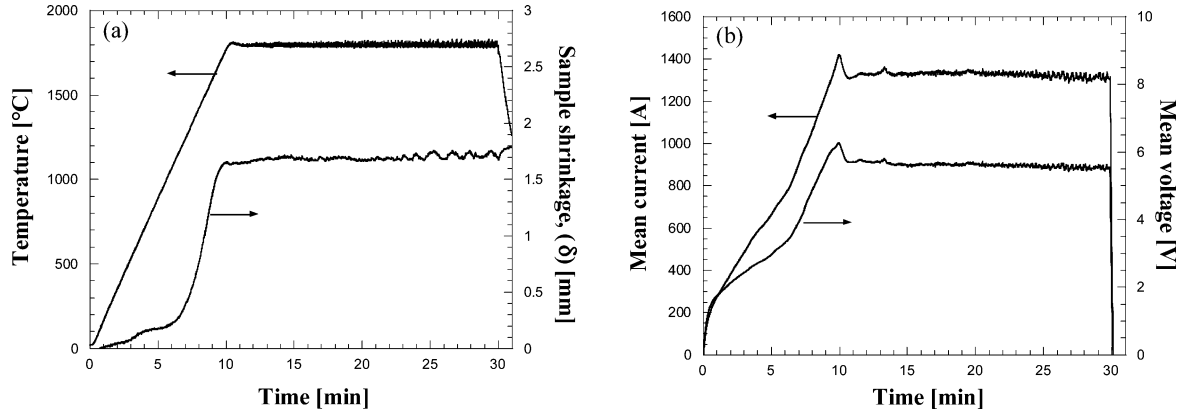

FIGURE 4. SPS outputs temporal profiles recorded during the fabrication of dense TaB_2−TaC−SiC: (a) temperature and sample shrinkage, (b) mean current intensity, and mean voltage (T_D = 1800 °C, t_H = 10 min, t_T = 30 min, P = 20 MPa).

temperature of the sample was in the range of about 1200−1700 °C. The displacement continued to increase at a slower rate until the T_D value was achieved, while less significant changes were evidenced from the corresponding profile during the isothermal stage. Nevertheless, products densities obtained after 30 min resulted about 4% (TS) and 1−2% (TTS) higher as compared to samples processed only during the 0−10 min time interval, thus indicating that sintering phenomena are still taking place. Such a behavior is similar to that observed when processing analogous Zr- (10, 11) and Hf-based (12) UHTCs. Regarding the electrical behavior of the system (cf. Figure 4b), it may be seen that to satisfy the selected thermal cycle, the current and voltage were augmented by the SPS apparatus controller during the nonisothermal heating (0−10 min). Afterward, both parameters rapidly decrease down to the corresponding stationary mean values, i.e., about 1340 A and 5.6 V, respectively.

The situation described above is also qualitatively representative of the experiments performed with the TS system. Thus, the considerations made for TTS hold also true for the binary system. Regarding the corresponding SPSed products density, a value of about 96% of the theoretical values was obtained in both cases.

3.3. Characterization of SPSed Products. Images a and b in Figure 5 show two backscattered SEM micrographs at different magnifications of the TS product sintered

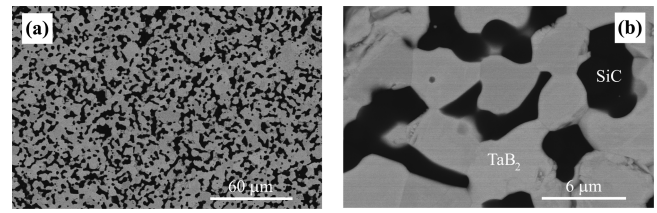

FIGURE 5. SEM backscattered micrographs of SPSed $2TaB_2$- SiC product: (a) 500× and (b) 5000×.

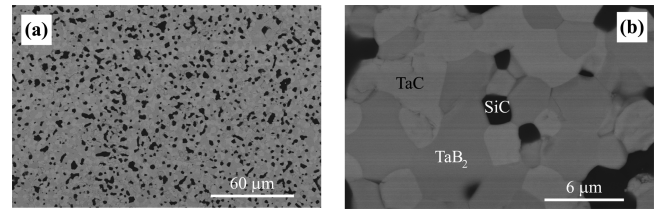

FIGURE 6. SEM backscattered micrographs of SPSed $4TaB_2$−4TaC−1.5SiC product: (a) 500× and (b) 5000×.

by SPS at 1800 °C for 30 min. The SiC (darker region) and TaB_2 (lighter zone) phases appear well-distributed throughout the sample. Analogously, two micrographs related to the TaB_2−TaC−SiC bulk product have been reported in images a and b in Figure 6, where three phases corresponding to the expected TaC (brighter), TaB_2 (medium bright), and SiC (darker) products according to reaction 2 are easily distinguishable. In particular, the relatively lower amount of SiC

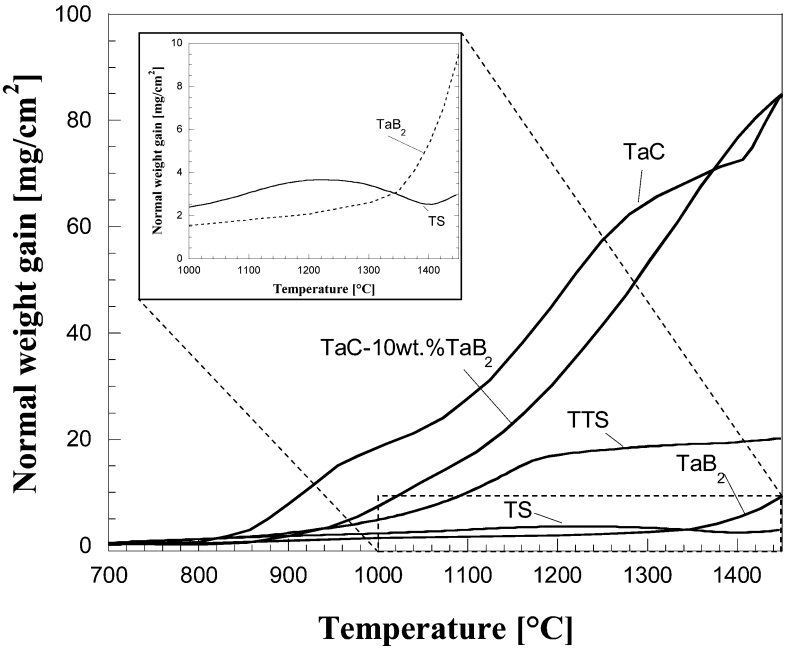

FIGURE 7. Comparison among specific weight changes as a function of temperature during nonisothermal TGA oxidation in air of TS, TTS sintered by SPS and other analogous Ta-based UHTC products (6).

present in the ternary bulk UHTC as compared to the binary composite is apparent from these figures. Moreover, the microstructure of TTS is finer and more homogeneous in comparison with that of TS. The grains size of each phase is generally <5 μm, i.e. slightly larger than the average grains size observed in SHS powders before sintering (cf. Figure 3b).

The oxidation resistances of the two composites synthesized and sintered in this work have been measured using TGA by monitoring their weight changes when subjected to an oxidizing environment (air) at high temperature. The results obtained during dynamic (nonisothermal) oxidation tests in the temperature range 700−1450 °C are reported in Figure 7 along with those reported in the literature relative to monolithic TaB_2 and TaC as well as the composite TaC−10 wt % TaB_2 (6). It is clearly seen that when SiC-free monolithic and composite Ta-based materials are exposed to O_2, mass gain monotonically increases with temperature in all cases, although their behavior is quantitatively different. Specifically, TaC and TaC−10 wt % TaB_2 start oxidizing quite rapidly at relatively low temperature level (about 850 °C), whereas, for the case of pure TaB_2, weight gain increases significantly only when temperature is higher than 1300 °C (see inset in Figure 7). Furthermore, the presence of SiC improves resistance to oxidation of the material. In particular, a relative maximum is displayed for the binary TS system at about 1200 °C, as clearly shown in the inset of Figure 7. Such oxidation behavior is also typically exhibited by other MB_2−SiC (M = Zr, Hf) systems reported in the literature, including those fabricated by means of the same processing route utilized in this work (10, 12), except for the mechanical activation. In fact, silicon carbide is responsible for the formation of a borosilicate protective layer, as discussed in details in several studies reported in the literature on this subject (5, 19−21). The role played by SiC in protecting the TS material to oxidation at high temperatures is particularly pronounced in the range 1350−1450 °C, where weight gain for pure TaB_2 becomes much more than twice with respect to the TS system. The fact that the latter one shows a normal weight gain slightly higher than TaB_2 at lower temperatures may be ascribed to the different relative densities of the two samples, i.e., about 96 and 98 % for the binary and single-phase systems, respectively. Thus, a slightly higher external surface area is exposed to air in the first case.

The lower resistance to oxidation manifested by the TTS system as compared to the TS is consistent with the corresponding behavior observed when analogous Hf-based binary and ternary composites are compared (12). This fact can be likely ascribed to two factors, i.e., the relatively lower SiC content, i.e., 13.7 and 27.9 vol %, for the TTS and TS samples, respectively, as well as to the presence of TaC, which appears to be detrimental as far as oxidation resistance is concerned. In fact, as clearly observed by the TGA results obtained by Zhang et al. (6) and reported in Figure 7 for the sake of comparison, TaC is very sensitive to the oxidative environment at high temperature. This is because it oxidizes rapidly to form various Ta oxides, mainly Ta_2O_5 and TaO, as clearly observed in Figure 8, where the XRD pattern of an oxidized TTS sample is reported, and carbon oxides. This event promotes the formation of a porous product which allows for the oxygen to diffuse through the bulk of the UHTC material, thus the latter one will keep oxidizing.

The mechanical properties (hardness and fracture toughness) of TS and TTS products obtained in this work by SPS at 1800 °C are included in Table 3 along with the corresponding values related to the analogous Ta-based materials recently investigated in the literature using different consolidation method (HP) and conditions (6, 8, 22). The

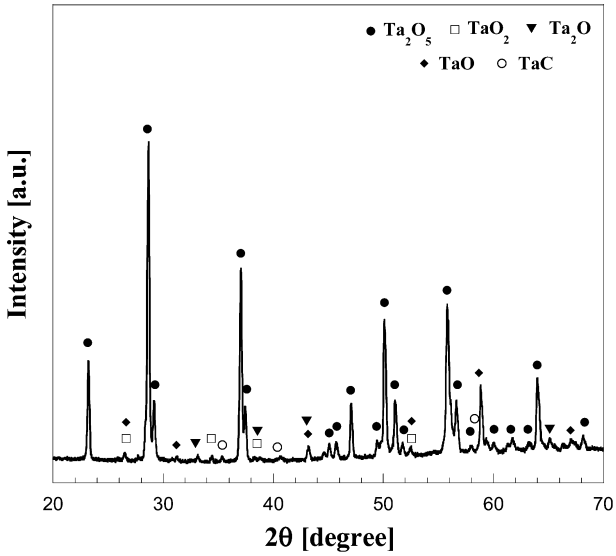

FIGURE 8. XRD pattern of TTS SPSed sample surface after being exposed to air at high temperature during nonisothermal TGA (cf. Figure 7).

reported results are consistent with the conclusion generally drawn when comparing other UHTCs, namely ZrB_2- and HfB_2-based, obtained by combining SHS and SPS techniques (10−12) with similar materials produced by other, more time and energy-consuming, alternative methods. It was found that the combination of SHS, as in situ synthesis route of composite powders, with a rapid consolidation technique (SPS) allows for the obtainment of bulk materials with properties generally comparable to, and in some cases superior to, those reported in the literature. This conclusion is confirmed in this study.

As already emphasized in previous papers (10−12), the benefits arising from the use of the SHS method could be ascribed to the improved sinterability of the resulting products as compared to powders obtained using other preparation routes. Mishra et al. (23) related the observed behavior to the higher defect concentration present in SHSed specimen, as a consequence of the drastic thermal conditions encountered during combustion synthesis, with respect to other methods. Furthermore, the higher densification level achieved under the same SPS conditions when consolidating ZrB_2−ZrC−SiC powders prepared by SHS instead of the purely blended ceramic constituents (11), was attributed to the relatively finer boride and carbide grains obtained in the first case, which cause a reduction of diffusion distances among the three ceramics constituents during sintering.

Regarding the properties reported in Table 3, it is seen that the fracture toughness value (K_{IC}) of the TS ceramic

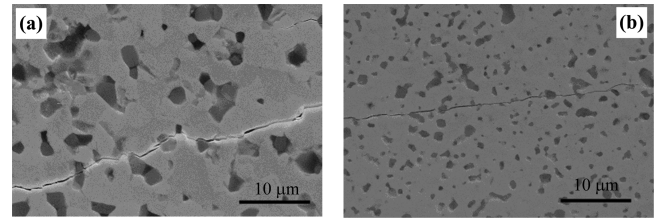

FIGURE 9. Crack propagation behavior in spark plasma sintered (a) $2TaB_2$−SiC and (b) $4TaB_2$−4TaC−1.5SiC samples.

fabricated in this work is much more higher than TTS as well as the other monolithic and composite products indicated in the table.

Further studies involving the TS and TTS systems were addressed to identify possible mechanisms for explaining the higher value of fracture toughness found, under the same indentation conditions, for the binary composite. The behavior of cracks formed on the two samples as a consequence of the application of 10 kg indentation loads is rather different, as observed from images a and b in Figure 9. Indeed, it can be clearly seen that the trajectory followed by the crack formed in TS sample (cf. Figure 9a) is relatively irregular, often intergranular, associated with an increase of its actual propagation path and, consequently, energy dissipation. Crack bridging, crack deflection, frictional interlocking, and crack branching are the more specific toughening mechanisms evidenced for this system during fracture analysis. Conversely, the trajectory of the crack that propagated across the TTS sample (cf. Figure 9b) appears much more regular. Only few evidence of crack bridging and frictional interlocking are found in this latter case. Such behavior is consistent with the relatively lower K_{IC} value obtained correspondingly. This finding could be likely ascribed to the relatively finer and more homogeneous microstructure, as compared to that displayed by the TS sample, that facilitates crack propagation.

4. SUMMARY AND CONCLUSIONS

The refractory TaB_2−SiC (2:1 molar ratio) and TaB_2−TaC−SiC (4:4:1.5 molar ratio) composites were synthesized in this work by SHS starting from Ta, B_4C, Si, and graphite powders, once mechanochemically activating the starting mixture for 20 min (ball to powders ratio equal to 1) to overcome diffusion limitation initially present in simply blended reaction promoters. The resulting powders were in both cases SPSed for a total processing time of 30 min by setting the dwell temperature to 1800 °C, heating rate to about 180 °C/min, the mechanical pressure to 20 MPa, and

Table 3. Properties of Bulk Ta-Based Refractory Composites

system	densification method (temperature)	relative density (%)	hardness (GPa) (applied load)	K_{IC} (MPa $m^{1/2}$)	ref
TaB_2	hot pressing[a] (2100 °C)	98	25.6 ± 0.7 (0.5 kg)	4.5 ± 0.3	(8)
TaC	hot pressing[a] (2300 °C)	94	14.1 ± 0.2 (0.5 kg)	3.5 ± 0.2	(6, 22)
TaC−TaB_2	hot pressing[a] (2100 °C)	98.6	19.4 ± 0.6 (0.5 kg)	3.4 ± 0.1	(6)
TS	spark plasma sintering (1800 °C)	∼96	18.9 ± 0.4 (10 kg)	8.4 ± 0.8	This work
TTS	spark plasma sintering (1800 °C)	∼96	18.3 ± 0.3 (10 kg)	4.2 ± 0.3	This work

[a] Graphite furnace.

nonisothermal heating time of 10 min, thus obtaining products about 96% dense.

Thermogravimetric analysis results evidenced the beneficial effect of SiC in the resistance to oxidation behavior of the composite materials, while the presence of TaC appears to be inconvenient from this point of view. In particular, the most significant improvement is observed in the binary system as compared to monolithic TaB_2 at temperature higher than 1350 °C. This finding is as a consequence of the formation of a borosilicate glass layer able to protect the bulk material.

The mechanical properties of the TS and TTS composites produced by SPS in the present investigation can be considered in general similar to those ones of TaB_2 and TaC, either in monolithic or composite bulk forms, densified by HP in a graphite furnace, although fracture toughness is significantly higher for the TaB_2−SiC sample. This result is also valid when the comparison is extended to the TTS material, as a consequence of the relatively finer and more homogeneous microstructure displayed by the latter system, that facilitates crack propagation. On the other hand, several toughening mechanisms (crack bridging, crack deflection, frictional interlocking, and crack branching) are involved when TS samples are subjected to the same indentation conditions.

As far as sintering conditions reported in Table 3 are examined, the densification temperature and the processing time are, in this work, lower and shorter, respectively, as compared to the HP technique. The observed benefits, as evidenced in previous works where the fabrication of bulk Zr- and Hf-based ceramics was addressed (10−12), can be also ascribed to the use of SHS as synthesis method that is able to provide powders with improved sinterability as compared to mixtures obtained by blending the ceramic constituents.

Acknowledgment. IM (Innovative Materials) S.r.l., Italy, is gratefully acknowledged for granting the use of SPS apparatus. The authors thank Eng. Leonardo Esposito (Centro Ceramico di Bologna, Italy) for performing hardness and fracture toughness measurements.

Note Added after ASAP Publication. This paper was published on the Web on June 21, 2010, with incorrect data in Table 2. The corrected version was reposted on July 15, 2010.

REFERENCES AND NOTES

(1) Upadhya, K.; Yang, J.-M.; Hoffman, W. P. *Am. Ceram. Soc. Bull.* **1997**, *76*, 51–56.
(2) Rapp, R. *Mater. Today* **2006**, *9* (5), 6.
(3) Fahrenholtz, W. G.; Hilmas, G. E.; Talmy, I. G.; Zaykoski, J. A. *J. Am. Ceram. Soc.* **2007**, *90*, 1347–1364.
(4) Talmy, I. G.; Zaykoski, J. A.; Opeka, M. M.; Dallek, S. *Electrochem. Soc. Proc.* **2001**, *12*, 144–158.
(5) Peng, F.; Speyer, R. F. *J. Am. Ceram. Soc.* **2008**, *91* (5), 1489–1494.
(6) Zhang, X.; Hilmas, G.; Fahrenholtz, W. G. *J. Am. Ceram. Soc.* **2008**, *91* (12), 4129–4132.
(7) Peng, F.; Berta, Y.; Speyer, R. F. *J. Mater. Res.* **2009**, *24* (5), 1855–1867.
(8) Zhang, X.; Hilmas, G. E.; Fahrenholtz, W. G. *Mater. Lett.* **2008**, *62* (27), 4251–4253.
(9) Yeh, C. L.; Chen, Y. L. *J. Alloys Compd.* **2009**, *478* (1−2), 163–167.
(10) Licheri, R.; Orrù, R.; Locci, A. M.; Cao, G. *Ind. Eng. Chem. Res.* **2007**, *46*, 9087–9096.
(11) Licheri, R.; Orrù, R.; Musa, C.; Cao, G. *Mater. Lett.* **2008**, *62*, 432–435.
(12) Licheri, R.; Orrù, R.; Musa, C.; Locci, A. M.; Cao, G. *J. Alloys Compd.* **2009**, *478* (1−2), 572–578.
(13) Orrù, R.; Licheri, R.; Locci, A. M.; Cincotti, A.; Cao, G. *Mater. Sci. Eng., R* **2009**, *63* (4−6), 127–287.
(14) Cincotti, A.; Licheri, R.; Locci, A. M.; Orrù, R.; Cao, G. *J. Chem. Technol. Biotechnol.* **2003**, *78* (2−3), 122–127.
(15) Matthews, F. L.; Rawlings, R. In *Composite Materials: Engineering and Science*; Chapman & Hall: London, 1994.
(16) Shetty, D. K.; Wright, I. G.; Mincer, P. N.; Clauer, A. H. *J. Mater. Sci.* **1985**, *20*, 1873–1882.
(17) Barin, I. In *Thermochemical Data of Pure Substances*; VCH Verlag: Weinheim, Germany,1989.
(18) Suryanarayana, C. *Prog. Mater Sci.* **2001**, *46*, 1–184.
(19) Tripp, W. C.; Davis, H. H.; Graham, H. C. *Am. Ceram. Soc. Bull.* **1973**, *52* (8), 612–616.
(20) Hinze, J. W.; Tripp, W. C.; Graham, H. C. *J. Electrochem. Soc.* **1975**, *122* (9), 1249–1254.
(21) Monteverde, F.; Bellosi, A. *J. Eur. Ceram. Soc.* **2005**, *25* (7), 1025–1031.
(22) Zhang, X.; Hilmas, G.; Fahrenholtz, W. G. *J. Am. Ceram. Soc.* **2007**, *90* (2), 393–401.
(23) Mishra, S. K.; Das, S.; Pathak, L. C. *Mater. Sci. Eng., A* **2004**, *364* (1−2), 249–255.

AM100211H